

# CFARnet: deep learning for target detection with constant false alarm rate

Tzvi Diskin, Yiftach Beer, Uri Okun and Ami Wiesel

**Abstract**—We consider the problem of learning detectors with a Constant False Alarm Rate (CFAR). Classical model-based solutions to composite hypothesis testing are sensitive to imperfect models and are often computationally expensive. In contrast, data-driven machine learning is often more robust and yields classifiers with fixed computational complexity. Learned detectors usually do not have a CFAR as required in many applications. To close this gap, we introduce CFARnet where the loss function is penalized to promote similar distributions of the detector under any null hypothesis scenario. Asymptotic analysis in the case of linear models with general Gaussian noise reveals that the classical generalized likelihood ratio test (GLRT) is actually a minimizer of the CFAR constrained Bayes risk. Experiments in both synthetic data and real hyper-spectral images show that CFARnet leads to near CFAR detectors with similar accuracy as their competitors.

**Index Terms**—hypothesis testing, deep learning.

## I. INTRODUCTION

The deep learning revolution has led many to apply machine learning methods to classical problems in all fields including statistics. Examples range from estimation [1–6] to detection [7–12]. Deep learning is a promising approach for developing high accuracy and low complexity alternatives when classical solutions are intractable. To facilitate this switch, we must ensure that the learned solutions are accurate but also satisfy other classical requirements. In this paper, we focus on learning detectors for composite hypothesis testing. We claim that current solutions deliver on their promises but lack the Constant False Alarm Rate (CFAR) requirement which is critical in many applications. To close this gap, we provide a framework for learning accurate CFAR detectors.

Detection theory begins with simple hypothesis testing where a detector must decide between two fully specified distributions. The classical solution is the Likelihood Ratio Test (LRT) which is optimal in terms of maximizing the detection probability subject to a false alarm constraint. Composite hypothesis testing is a more challenging setting where the hypotheses involve unknown deterministic parameters. A CFAR detector is invariant to these parameters and has constant false alarm probabilities. This allows the user to set the thresholds a priori. A popular approach is the Generalized Likelihood Ratio Test (GLRT) which can be interpreted as estimating the unknown parameters and then plugging them into a standard LRT. GLRT performs well when the number of unknowns is relatively small and is asymptotically CFAR. In finite sample settings, however, it is generally sub-optimal. Additionally, it may be computationally expensive. Some techniques were

developed for designing CFAR detectors for specific families of distributions [13–15].

Data-driven classifiers are the machine learning counterpart to model-based detectors. In simple settings with no unknown deterministic parameters, it is well known that the optimal Bayes classifier converges to the LRT with a specific false alarm rate [16, p. 78]. More advanced classifiers can also maximize the cumulative detection rate over a wide range of false alarms, also known as the (partial) area under the curve (AUC) [17–19]. Large deviation analysis is available in [20]. Consequently, there is a growing body of works on using machine learning for target detection. In the context of hyper-spectral imagery, [11] introduced the use of support vector machines (SVM) and deep neural networks were proposed in [8]. In the context of radar detection, SVMs were considered in [10]. Specific CFAR radar detectors were developed by relying on CFAR features [21–23].

The main contribution of this paper is a framework for learning CFAR detectors, denoted as CFARnet. The framework is general purpose and can be applied to arbitrary composite hypothesis testing problems. CFARnet is based on adding a penalty function that decreases the distances between the distributions under different parameter values. To optimize CFARnet, we rely on empirical and differentiable distances that have recently become popular in unsupervised deep learning [24–26]. Theoretically, we prove that under asymptotic linear and Gaussian settings, GLRT is indeed a minimizer of the Bayes risk subject to a CFAR constraint. Practically, CFARnet is a differentiable approximation to this minimizer that can also be applied in more general settings.

Our experiments show that CFARnet is approximately CFAR while paying a small price in terms of accuracy. First, we show this in the context of detecting a signal with unknown amplitude in non-Gaussian noise. Next, we turn to a more challenging adaptive detection problem with unknown Gaussian noise covariance but access to secondary data of noise-only samples, which can be used for estimation of the covariance of the noise. [27–30]. Interestingly, we show that the popular regularizing trick, also known as shrinkage or diagonal loading, improves detection accuracy but leads to non-CFAR detectors. Using CFARnet, we learn a network which is both accurate and CFAR. Finally, we demonstrate the advantages of CFARnet in target detection of a plastic material in real hyperspectral imagery. Here too, CFARnet finds a tradeoff between accuracy and CFAR. Its advantages are evident when we examine the detection rates under a strict worst-case false alarm across the full image.

For completeness, we note that the CFAR notion is closely related to the topics of “fairness” and “out of distribution (OOD)” generalization which have recently attracted considerable attention in the machine learning literature, e.g., [31, 32]. CFAR can be interpreted as a fairness property with respect to the unknown deterministic parameters. The closest work is [33] which also enforces “equalized odds” using a distance between distributions. A main difference is that CFAR is a one-sided fairness property and requires equal rates only in the null hypothesis. Algorithmically, [33] compares the high dimensional joint distribution of the predictions and the unknown parameters, whereas we only consider the scalar distribution of the predictions. This makes our method significantly cheaper in terms of computational complexity. Indeed, we rely on a simple kernel based distance and do not require sophisticated adversarial networks.

## II. PROBLEM FORMULATION

We consider a binary hypothesis test. Let  $\mathbf{x}$  be an observed random vector whose distribution  $p(\mathbf{x}; \mathbf{z})$  depends on an unknown deterministic parameter  $\mathbf{z}$ . The value of  $\mathbf{z}$  defines two possible hypotheses

$$\begin{aligned} y = 0 : & \quad \mathbf{z} \in \mathcal{Z}_0 \\ y = 1 : & \quad \mathbf{z} \in \mathcal{Z}_1. \end{aligned} \quad (1)$$

A classical example is the following setting:

**Example 1.** *Target detection when both the target amplitude and the noise scaling are unknown:*

$$\mathbf{x} = A\mathbf{1} + \sigma\mathbf{n} \quad (2)$$

where  $\mathbf{1}$  is a target vector of ones,  $\mathbf{n}$  is a random vector with i.i.d. noise variables,  $\mathbf{z} = [A, \sigma]$  are deterministic unknown parameters, and

$$\begin{aligned} \mathcal{Z}_0 &= \{\mathbf{z} : A = 0, 0.5 \leq \sigma \leq 1\} \\ \mathcal{Z}_1 &= \{\mathbf{z} : A \neq 0, -1 \leq A \leq 1, 0.5 \leq \sigma \leq 1\} \end{aligned} \quad (3)$$

Here,  $A$  acts as a discriminative parameter that varies between the two hypotheses, whereas the noise variance  $\sigma^2$  is an unknown nuisance parameter which is identical in both.

The goal is to design a detector  $\hat{y}(\mathbf{x}) \in \{0, 1\}$  as a function of  $\mathbf{x}$  that will identify the true hypothesis  $y \in \{0, 1\}$ . Performance is measured in terms of probability of correct detection, also known as True Positive Rate (TPR):

$$\text{Pr}_{\text{TPR}}(\mathbf{z}) = \text{Pr}(\hat{y}(\mathbf{x}) = 1; y = 1) \quad (4)$$

and probability of false alarm, also known as False Positive Rate (FPR):

$$\text{Pr}_{\text{FPR}}(\mathbf{z}) = \text{Pr}(\hat{y}(\mathbf{x}) = 1; y = 0). \quad (5)$$

In practice, the user typically provides a false alarm constraint  $\text{Pr}_{\text{FPR}} \leq \alpha$  that must be satisfied and the goal is to maximize  $\text{Pr}_{\text{TPR}}$ .

It is standard to consider decision functions of the form

$$\hat{y}(\mathbf{x}) = \mathbf{1}_{T(\mathbf{x}) \geq \gamma} = \begin{cases} 0 & T(\mathbf{x}) < \gamma \\ 1 & T(\mathbf{x}) \geq \gamma \end{cases} \quad (6)$$

where  $T(\mathbf{x})$  is denoted as the **detector** function and  $\gamma$  is a **threshold** value. This structure allows users to tune the FPR by adjusting the threshold. Performance is usually visualized using the Receiver Operating Characteristic (ROC) which plots the TPR as a function of the FPR. In signal processing applications, users are often interested in a region of very low FPRs, e.g.,  $10^{-1} - 10^{-3}$  and the goal is to maximize the TPR probabilities in this area. A main challenge in detection theory is the unknown nuisance parameters under the null hypothesis  $y = 0$ , e.g., the unknown noise variance  $\sigma^2$  in Example 1. The false alarm probability (FPR) is generally a function of these parameters and cannot be controlled without their knowledge. Therefore, it is often preferable to restrict the attention to CFAR detectors.

**Definition 1.** *A detector  $T(\mathbf{x})$  is CFAR if its FPR  $\text{Pr}(T(\mathbf{x}) > \gamma | \mathbf{z} \in \mathcal{Z}_0)$  is invariant to the value of  $\mathbf{z} \in \mathcal{Z}_0$ , for any threshold  $\gamma$ .*

It is straightforward to see that the above definition is equivalent to invariance of the distribution of  $T(\mathbf{x})$  to all  $\mathbf{z} \in \mathcal{Z}_0$ . For example, in Example 1 above,  $T(\mathbf{x})$  is a CFAR test if its distribution is invariant to the value of  $\sigma^2$ .

As we will review below, many classical detectors are CFAR or asymptotically CFAR. With the growing trend of switching to machine learning, the goal of this paper is to introduce a framework for learning CFAR detectors, that can be used when classical detectors are intractable or far from optimal.

## III. EXISTING DETECTORS

### A. Classical detectors

Traditionally, detectors were developed using likelihood ratios. In the simple case, all the parameters of the hypotheses are known. For example, this is the case of target detection in (2) where,  $\mathcal{Z}_0 = \{\mathbf{z} : A = 0, \sigma = 1\}$  and  $\mathcal{Z}_1 = \{A = 1, \sigma = 1\}$ . In this case, hypothesis testing has an optimal solution known as the Likelihood Ratio Test (LRT) due to Neyman-Pearson lemma [16, p. 65]:

$$T_{\text{LRT}}(\mathbf{x}) = 2 \log \frac{p(\mathbf{x}; \mathbf{z} = \mathbf{z}_1)}{p(\mathbf{x}; \mathbf{z} = \mathbf{z}_0)} \quad (7)$$

where the threshold  $\gamma$  is chosen to satisfy the false alarm (FPR) constraint.

The more realistic scenario is composite hypotheses testing where one or both of the hypotheses allow multiple possible values and there is no solution which is optimal for all of them. A popular heuristic is the Generalized Likelihood Ratio Test (GLRT) that estimates the unknowns using the Maximum Likelihood (ML) technique and plugs them into the LRT detector [16, p. 200]:

$$T_{\text{GLRT}}(\mathbf{x}) = 2 \log \frac{\max_{\mathbf{z} \in \mathcal{Z}_1} p(\mathbf{x}; \mathbf{z})}{\max_{\mathbf{z} \in \mathcal{Z}_0} p(\mathbf{x}; \mathbf{z})} \quad (8)$$

Setting the threshold to ensure a fixed  $\text{Pr}_{\text{FPR}}$  is not trivial. Fortunately, under regularity conditions, GLRT is asymptotically CFAR and its threshold can be set for all values of the unknown parameters simultaneously.

GLRT is probably the most popular solution to composite hypothesis testing. It gives a simple recipe that performs well under asymptotic conditions. Its main downsides are that it is sensitive to deviations from its theoretical model, it is generally sub-optimal under finite sample settings and that it may be computationally expensive. Both the numerator and denominator of the GLRT involve optimization problems that may be large scale, non-linear and non-convex. Therefore, there is an ongoing search for robust and low cost alternatives.

### B. Learned detectors

An alternative approach to designing detectors is based on machine learning. The starting point to any data-driven learning is a training set. Hypothesis testing relies on a probabilistic model  $p(\mathbf{x}; \mathbf{z})$  and we need to use this model in order to generate a synthetic dataset. Hybrid settings involving a mixture of real and artificial samples are also common. For example, it is standard to plant synthetic targets on real noise or clutter samples [11].

A main challenge in generating data is that  $y \in \{0, 1\}$  and  $\mathbf{z}$  are not random variables but deterministic parameters without any prior distribution. A natural heuristic is to assume uniform fake priors, e.g., choose half of labels as  $y = 0$  and half as  $y = 1$  and assume that  $\mathbf{z}$  is uniformly distributed on its corresponding domains. For each  $y_i$  and  $\mathbf{z}_i$ , we then generate a measurement  $\mathbf{x}_i$  according to the true  $p(\mathbf{x}; \mathbf{z}_i)$  and obtain a synthetic dataset

$$\mathcal{D}_N = \{\mathbf{x}_i, \mathbf{z}_i, y_i\}_{i=1}^N. \quad (9)$$

Next, a class of possible detectors  $\mathcal{T}$  is chosen in order to tradeoff expressive power with computational complexity in test time. The class is usually a fixed differentiable neural network architecture. In our context, it also makes sense to reuse existing ingredients from classical detector as non-linear features or internal sub-blocks [7, 23].

Finally, the learned detector is defined as the minimizer of an empirical loss function

$$\min_{\hat{T} \in \mathcal{T}} \frac{1}{N} \sum_{i=1}^N L(\hat{T}(\mathbf{x}_i), y_i). \quad (10)$$

where  $L(\cdot; \cdot)$  is a classification loss function. Ideally, we would like to minimize the zero-one loss which corresponds to the average probability of error. Practically, for efficient optimization, a smooth and convex surrogate loss, as the hinge or cross entropy functions, is preferable. The overall procedure for learning a detector is summarized in Algorithm 1.

Learned detectors have strong theoretical guarantees in simple testing problems where  $y$  uniquely defines  $\mathbf{z}$ . With a sufficiently expressive class of detectors and a large enough

---

### Algorithm 1 NET detector for $p(\mathbf{x}; \mathbf{z})$

---

- Choose  $\text{Pr}^{\text{fake}}(y)$ .
  - Choose  $p^{\text{fake}}(\mathbf{z}; y)$ .
  - For each  $i = 1, \dots, N$ :
    - Generate  $y_i$ .
    - Generate  $\mathbf{z}_i$  given  $y_i$ .
    - Generate  $\mathbf{x}_i$  given  $\mathbf{z}_i$ .
  - Solve
 
$$\min_{\hat{T} \in \mathcal{T}} \frac{1}{N} \sum_{i=1}^N L(\hat{T}(\mathbf{x}_i), y_i).$$
- 

training set, minimizing the zero-one loss leads to the Bayes optimal detector. It is identical to the LRT with the threshold

$$\gamma = 2 \log \left( \frac{\text{Pr}^{\text{fake}}(y=0)}{\text{Pr}^{\text{fake}}(y=1)} \right). \quad (11)$$

Minimizers of Bayes risk consistent surrogates, as the hinge loss, also asymptotically converge to this LRT [34]. Thus, any simple LRT can be approximated by tuning  $\text{Pr}^{\text{fake}}(y)$  to achieve a desired FPR.

There is limited theory on the performance of learned detectors in composite hypothesis testing. Numerical experiments suggest that learned detectors usually provide similar accuracy as their corresponding (G)LRTs. On the negative side, our experiments show that learned detectors are not CFAR and result in significantly different false alarm rates for different values of  $\mathbf{z} \in \mathcal{Z}_0$ . To close this gap, in the next section we propose a framework for learning CFAR detectors.

## IV. LEARNING CFAR DETECTORS

In this section, we introduce CFARnet, a framework for designing CFAR detectors using machine learning. CFARnet introduces two modifications to Algorithm 1. First, we augment the classification loss with a penalty function that ensures similar distributions of the detector  $\hat{T}(\mathbf{x})$  for all values of  $\mathbf{z} \in \mathcal{H}_0$ . Second, in order to compare such distributions empirically, we need to generate multiple  $\{\mathbf{x}_{ij}\}_{j=1}^M$  for each  $\mathbf{z}_i$ .

The main idea is adding a penalty to the objective function that promotes a CFAR detector. For this purpose, we need to measure the distance between different distributions.

**Definition 2.** Let  $X \sim p(X)$  and  $Y \sim p(Y)$  be two random variables. A statistical distance  $d(X; Y)$  is a function that satisfies  $d(X; Y) \geq 0$  with equality if and only if  $p(X) = p(Y)$ . In particular, an integral probability metric  $d(X; Y)$  can be empirically estimated using a set of data realizations  $\hat{d}(\{\mathbf{X}_j\}_{j=1}^M, \{\mathbf{Y}_j\}_{j=1}^M)$ .

Given a statistical distance  $d(\cdot; \cdot)$ , the penalty is defined as a sum of distances between the distributions of  $\hat{T}$  under different values of  $\mathbf{z}$ :

$$R(\hat{T}) = \sum_{\mathbf{z}, \mathbf{z}' \in \mathcal{Z}_0} d(\hat{T}(\mathbf{x}); \hat{T}(\mathbf{x}')) \quad (12)$$

where

$$\begin{aligned} \mathbf{x} &\sim p(\mathbf{x}; \mathbf{z}) \\ \mathbf{x}' &\sim p(\mathbf{x}; \mathbf{z}'). \end{aligned} \quad (13)$$

Clearly, any CFAR test must satisfy  $R(\hat{T}) = 0$ .

Practically, to minimize (12), we use empirical estimates of the distances where each distribution is represented using a small dataset. For each  $\mathbf{z}_i$ , we synthetically generate multiple observations  $\mathbf{x}_{ij}$  for  $j = 1, \dots, M$ . Similarly, for each  $\mathbf{z}_{i'}$  we compute multiple  $\mathbf{x}'_{ij}$ . We then plug these into the empirical distances:

$$\hat{R}(\hat{T}) = \sum_{i, i'} \hat{d} \left( \{\hat{T}(\mathbf{x}_{ij})\}_{j=1}^M; \{\hat{T}(\mathbf{x}'_{ij})\}_{j=1}^M \right) \quad (14)$$

Our implementation of CFARnet uses the Maximum Mean Discrepancy (MMD) distance [26] as detailed in Appendix A. We also use a hyper-parameter  $\alpha > 0$  that trades off the importance of the classification accuracy versus the CFAR penalty. The overall CFARnet procedure is summarized in Algorithm 2.

---

**Algorithm 2** CFARnet detector for  $p(\mathbf{x}; \mathbf{z})$

---

- Choose  $\Pr^{\text{fake}}(y)$ .
  - Choose  $p^{\text{fake}}(\mathbf{z}; y)$ .
  - For each  $i = 1, \dots, N$ :
    - Generate  $y_i$ .
    - Generate  $\mathbf{z}_i$  given  $y_i$ .
    - For  $j = 1, \dots, M$ :
      - Generate  $\mathbf{x}_{ij}$  given  $\mathbf{z}_i$ .
  - Solve
 
$$\min_{\hat{T} \in \mathcal{T}} \frac{1}{N} \sum_{i=1}^N L(\hat{T}(\mathbf{x}_i), y_i) + \alpha \hat{R}(\hat{T}).$$
- 

## V. RELATION TO GLRT

A natural question is the relation between the learned CFARnet detector and the classical GLRT. To answer it we consider a theoretical version of CFARnet which minimizes the expected Bayesian 0-1 loss subject to an exact CFAR constraint:

$$\text{BayesCFAR} : \begin{cases} \min_{\hat{T}, \gamma} & \Pr(\mathbf{1}_{T \geq \gamma} \neq y) \\ \text{s.t.} & \hat{T} \text{ is CFAR} \end{cases} \quad (15)$$

where the fake priors enter the optimization through the error probability. CFARnet with large  $\alpha$  is a finite sample differentiable approximation of BayesCFAR. The main result of this section is that under favorable conditions, GLRT is a minimizer of BayesCFAR. Thus, CFARnet can be interpreted as a deep learning approximation to GLRT, which can be learned even when the latter is intractable (due to unknown models or high computational complexity). We conjecture that this relation holds for most settings in which GLRT attains its asymptotic performance. In what follows, we rigorously prove this claim for the general Gaussian linear problem.

**Definition 3.** *The linear model with Gaussian noise model is defined as*

$$\mathbf{x} = \mathbf{H}\mathbf{z}_r + \mathbf{n} \quad (16)$$

where  $\mathbf{x} \in \mathbb{R}^n$  is the observed vector,  $\mathbf{H} \in \mathbb{R}^{n \times d_r}$  is a known matrix with full column rank. The model involves two types of deterministic parameters:  $\mathbf{z}_r \in \mathbb{R}^{d_r}$  is an unknown signal and  $\mathbf{n}$  is a noise vector distributed as

$$\mathbf{n} \sim \mathcal{N}(\mathbf{0}, \Sigma(\mathbf{z}_n)) \quad (17)$$

where  $\mathbf{z}_n \in \mathbb{R}^{d_n}$  is a nuisance parameter. The goal is to test the presence of a non-zero signal  $\mathbf{z}_r$ :

$$\begin{aligned} y = 0 : & \quad \mathbf{z}_r = \mathbf{0} \\ y = 1 : & \quad \mathbf{z}_r \neq \mathbf{0}. \end{aligned} \quad (18)$$

Note that the above Gaussian linear model is very general and allows **arbitrary noise covariance with any nuisance parameters**. Computing GLRT in such models is typically intractable and involves the solution of two challenging optimization problems in inference time as detailed in (8). In contrast, evaluating CFARnet is straight forward.

To compare GLRT with BayesCFAR, we define the following fictitious priors:

- The prior over  $\mathbf{z}_r$  is Gaussian:  $p^{\text{fake}}(\mathbf{z}_r) \sim \mathcal{N}(0, \sigma_r^2 \mathbf{I})$ .
- The prior over  $\mathbf{z}_n$  is any non-zero density  $p^{\text{fake}}(\mathbf{z}_n)$ .
- The prior over  $y$  is  $\Pr^{\text{fake}}(y = 0) = p_0 > 0$ .

To simplify the presentation, we provide two equivalence results. The first theorem is based on the assumption that  $\mathbf{z}_n$  is known and available as a secondary input to the detectors. In this situation,  $T_{\text{GLRT}}(\mathbf{x}, \mathbf{z}_n)$  is based on the true  $\mathbf{z}_n$  and an ML estimate of  $\mathbf{z}_r$ . In BayesCFAR, the detector may depend on  $\mathbf{z}_n$  but the objective is still averaged with respect to it. This result is non-asymptotic. It is based on the CFAR property of the linear Gaussian GLRT and can be extended to other non-Gaussian settings in which GLRT is CFAR.

**Theorem 1.** *Consider the linear Gaussian model with a large enough  $\sigma_r^2$  and a **known**  $\mathbf{z}_n$ , then there exists a threshold  $\gamma$  such that GLRT solves BayesCFAR.*

*Proof.* The proof contains three main steps: (a) we show that GLRT is equal to the LRT where  $\mathbf{z}_r$  is random with a sufficiently large  $\sigma_r$  up to a term that depends only on  $\mathbf{z}_n$ . (b) we show that for a given rate of FPR, both detectors achieve the maximal TPR for any value of  $\mathbf{z}_n$ . (c) we use this fact to show that the GLRT with the right threshold minimizes the Bayesian 0-1 loss among all the detectors that have constant FPR over all values of  $\mathbf{z}_n$ .

Step (a): when  $\mathbf{z}_r$  is random and  $\mathbf{z}_n$  is known, the problem reduces to a simple hypothesis test

$$\begin{aligned} y = 0 : & \quad \mathbf{x} \sim \mathcal{N}(\mathbf{0}, \Sigma) \\ y = 1 : & \quad \mathbf{x} \sim \mathcal{N}(\mathbf{0}, \Sigma + \sigma_r^2 \mathbf{H}\mathbf{H}^T), \end{aligned} \quad (19)$$

where  $\Sigma = \Sigma(\mathbf{z}_n)$ . We denote its LRT by PBL (Partially Bayesian LRT) which is given by (see Appendix B):

$$\begin{aligned} T_{\text{PBL}}(\mathbf{x}, \mathbf{z}_n) &= 2 \log \left( \frac{p(\mathbf{x}|y=1)}{p(\mathbf{x}|y=0)} \right) \\ &= \mathbf{x}^T \Sigma^{-1} \mathbf{H} \left( \mathbf{H}^T \Sigma^{-1} \mathbf{H} + \frac{1}{\sigma_r^2} \mathbf{I} \right)^{-1} \mathbf{H}^T \Sigma^{-1} \mathbf{x} \\ &\quad + \log \left( \frac{\det \Sigma}{\det \left( \Sigma + \sigma_r^2 \mathbf{H} \mathbf{H}^T \right)} \right). \end{aligned} \quad (20)$$

Meanwhile, the GLRT is given by (see Appendix C):

$$T_{\text{GLRT}}(\mathbf{x}, \mathbf{z}_n) = \mathbf{x}^T \Sigma^{-1} \mathbf{H} \left( \mathbf{H}^T \Sigma^{-1} \mathbf{H} \right)^{-1} \mathbf{H}^T \Sigma^{-1} \mathbf{x}. \quad (21)$$

Therefore, for large enough  $\sigma_r$ , the  $\frac{1}{\sigma_r^2}$  term in (20) vanishes and PBL converges to GLRT up to a term that depends only on  $\mathbf{z}_n$ :

$$T_{\text{PBL}}(\mathbf{x}, \mathbf{z}_n) = T_{\text{GLRT}}(\mathbf{x}, \mathbf{z}_n) + c(\mathbf{z}_n), \quad (22)$$

where

$$c(\mathbf{z}_n) = \log \left( \frac{\det \Sigma}{\det \left( \Sigma + \sigma_r^2 \mathbf{H} \mathbf{H}^T \right)} \right). \quad (23)$$

This is reminiscent of the ML and JMAP-ML relation in [35].

Step (b): we now show that despite the  $c(\mathbf{z}_n)$  term, if we constrain the detectors to have an FPR of  $\alpha$  for any value  $\mathbf{z}_n$ , then both detectors and their thresholds are equivalent. Because  $\mathbf{z}_n$  is known, the thresholds  $\gamma_{\text{PBL}}$  can depend on  $\mathbf{z}_n$ , and are given implicitly by:

$$\alpha = \int_{\gamma_{\text{PBL}}}^{\infty} p_{\text{PBL}}^0(\tau, \mathbf{z}_n) d\tau, \quad (24)$$

where  $p_{\text{PBL}}^0$  is the PDF of  $T_{\text{PBL}}(\mathbf{x}, \mathbf{z}_n)$  for a given  $\mathbf{z}_n$ , under the  $y = 0$  hypothesis. Similarly, the threshold of the GLRT is given implicitly by:

$$\alpha = \int_{\gamma_{\text{GLRT}}}^{\infty} p_{\text{GLRT}}^0(\tau) d\tau, \quad (25)$$

where  $p_{\text{GLRT}}^0$  is the PDF of  $T_{\text{GLRT}}(\mathbf{x}, \mathbf{z}_n)$  for a given  $\mathbf{z}_n$ , under the  $y = 0$  hypothesis. As the PDF of the GLRT does not depend on  $\mathbf{z}_n$  [page](#) [16], the threshold also does not depend on  $\mathbf{z}_n$ . Using (22), the PDFs of the detectors satisfy:

$$p_{\text{PBL}}^0(\tau - c(\mathbf{z}_n), \mathbf{z}_n) = p_{\text{GLRT}}^0(\tau) \quad (26)$$

and thus

$$\begin{aligned} \int_{\gamma_{\text{GLRT}}}^{\infty} p_{\text{GLRT}}^0(\tau) d\tau &= \int_{\gamma_{\text{PBL}}}^{\infty} p_{\text{PBL}}^0(\tau - c(\mathbf{z}_n), \mathbf{z}_n) d\tau \\ &= \int_{\gamma_{\text{PBL}} + c(\mathbf{z}_n)}^{\infty} p_{\text{PBL}}^0(\tau, \mathbf{z}_n) d\tau. \end{aligned} \quad (27)$$

From (27) it can be seen the thresholds of the two detectors are related by:

$$\gamma_{\text{GLRT}}(\alpha) = \gamma_{\text{PBL}}(\alpha, \mathbf{z}_n) + c(\mathbf{z}_n). \quad (28)$$

Thus, by the Neyman-Pearson Lemma, PBL, and thus also the identical GLRT, maximize the TPR for any FPR  $\alpha$  and any nuisance parameter  $\mathbf{z}_n$ .

Step (c): it remains to show that GLRT with the right threshold solves BayesCFAR. We denote the FPR of a test  $(T(\mathbf{x}, \mathbf{z}_n), \gamma)$  for a given  $\mathbf{z}_n$  by:

$$\alpha(T, \gamma, \mathbf{z}_n) = \Pr(T(\mathbf{x}, \mathbf{z}_n) > \gamma | y = 0, \mathbf{z}_n), \quad (29)$$

and similarly the false negative rate (which is 1-TPR):

$$\beta(T, \gamma, \mathbf{z}_n) = \Pr(T(\mathbf{x}, \mathbf{z}_n) < \gamma | y = 1, \mathbf{z}_n). \quad (30)$$

The objective of BayesCFAR is therefore:

$$L_{0-1}(T, \gamma) = p_0 \mathbb{E}[\alpha(T, \gamma, \mathbf{z}_n)] + p_1 \mathbb{E}[\beta(T, \gamma, \mathbf{z}_n)], \quad (31)$$

where the expectations are over  $p^{\text{fake}}(\mathbf{z}_n)$ .

Now we show that the GLRT with a threshold  $\gamma$  that is generally a function of  $\mathbf{H}$  and the priors over  $\mathbf{z}_n$  and  $y$ , is a solution (15) which can be written as:

$$\begin{aligned} \min_{T(\mathbf{x}, \mathbf{z}_n), \gamma} \quad & L_{0-1}(T, \gamma) \\ \text{s.t.} \quad & \alpha(T, \tilde{\gamma}, \mathbf{z}_n) = \alpha(T, \tilde{\gamma}, \mathbf{z}'_n) \quad \forall \mathbf{z}_n, \mathbf{z}'_n, \tilde{\gamma}, \end{aligned} \quad (32)$$

Note that the constraint must be satisfied for all  $\tilde{\gamma}$  and not just for the optimal  $\gamma$ .

Due to the CFAR constraint, the FPR is constant with respect to  $\mathbf{z}_n$  and so is its expectation:

$$\mathbb{E}[\alpha(T, \gamma, \mathbf{z}_n)] = \alpha(T, \gamma), \quad (33)$$

where  $\alpha(T, \gamma)$  is the FPR of the test on any value of  $\mathbf{z}_n$ . Thus the Bayesian 0-1 loss can be written as:

$$L_{0-1}(T, \gamma) = p_0 \alpha(T, \gamma) + p_1 \mathbb{E}[\beta(T, \gamma, \mathbf{z}_n)]. \quad (34)$$

The best threshold for any detector can be therefore found by minimizing (34) with respect to  $\gamma$ . Specifically we denote the optimal threshold of the GLRT detector by  $\gamma^*$ , and denote the corresponding FPR as  $\alpha^*$ .

Now we prove that any other CFAR detector gives a larger or equal Bayesian 0-1 loss. We assume that there exist a detector  $(T'(\mathbf{x}, \mathbf{z}_n), \gamma')$  that has FPR of  $\alpha'$  for any value of  $\mathbf{z}_n$ . Its Bayesian loss is given by:

$$\begin{aligned} L_{0-1}(T', \gamma') &= p_0 \alpha' + p_1 \mathbb{E}[\beta(T', \gamma', \mathbf{z}_n)] \\ &\geq p_0 \alpha' + p_1 \mathbb{E}[\beta(T_{\text{GLRT}}, \gamma'_{\text{GLRT}}, \mathbf{z}_n)] \\ &= L_{0-1}(T_{\text{GLRT}}, \gamma'_{\text{GLRT}}) \\ &\geq L_{0-1}(T_{\text{GLRT}}, \gamma^*), \end{aligned} \quad (35)$$

where  $\gamma'_{\text{GLRT}}$  is the threshold that gives FPR of  $\alpha'$  to the GLRT. The first inequality is due to the optimality of GLRT among detectors that have FPR  $\alpha'$  for any value of  $\mathbf{z}_n$ . The second inequality is due to the optimality of the threshold  $\gamma^*$  for the GLRT detector.

In conclusion, the GLRT with threshold  $\gamma^*$  gives the minimum Bayesian loss among all the detectors that have constant false alarm rate over  $\mathbf{z}_n$ .  $\square$

The second theorem considers the more challenging case in which  $\mathbf{z}_n$  is unknown. In this case, the GLRT  $\tilde{T}_{\text{GLRT}}(\mathbf{x})$

uses ML to estimate both  $\mathbf{z}_r$  and  $\mathbf{z}_n$ . The result is based on the asymptotic properties of GLRT (but can be extended to non-Gaussian settings).

**Theorem 2.** *Consider the linear Gaussian model with a large enough  $\sigma_r^2$  and unknown  $\mathbf{z}_n$ , then if  $n \gg \max\{d_r, d_n\}$ , there exists a threshold  $\gamma$  such that GLRT solves BayesCFAR.*

*Proof.* Under large data records, GLRT attains its asymptotic distribution as defined in [16, (6.24)]. When the Fisher information matrix is block diagonal, this distribution is identical to that without (or with known) nuisance parameters as defined in [16, (6.27)]. Thus,

$$L_{0,1}(\tilde{T}_{\text{GLRT}}, \gamma^*) = L_{0,1}(T_{\text{GLRT}}, \gamma^*), \quad (36)$$

and  $\tilde{T}_{\text{GLRT}}(\mathbf{x})$  satisfies the CFAR constraint. A detector that does not use  $\mathbf{z}_n$  as input cannot be better than the optimal detector that uses  $\mathbf{z}_n$  as input. Thus, the GLRT with unknown  $\mathbf{z}_n$  and the threshold  $\gamma^*$  is the minimizer of the Bayesian 0-1 loss among CFAR detectors.

It remains to clarify what exactly are the conditions for large data records. The assumptions in [16, p. 206] are: large data, weak signal and that the MLE attains its asymptotic density. The first and third assumptions are satisfied in the Gaussian case when  $n \gg \max\{d_r, d_n\}$ . In appendix D, we prove that the assumption of weak signal is not necessary in our setting.  $\square$

The theorems give more insight on CFARnet as a deep learning approximation of BayesCFAR. In the asymptotic Gaussian setting, GLRT is CFAR and there is no degradation in ROC performance due to the additional constraint. This holds for Gaussian models with arbitrary covariance structures. More generally, there is an inherent tradeoff between accuracy and CFAR and a sweet spot must be identified for each application. The theorems also gives a new interpretation to the GLRT, Wald and Rao tests, that have the same asymptotic distributions [16, p. 205] but do not directly minimize any cost function. Apparently, in asymptotic Gaussian linear models, they are the minimizers of the Bayesian 0-1 loss subject to the CFAR constraint.

## VI. NUMERICAL EXPERIMENTS

In this section, we demonstrate the advantages of CFARnet via numerical experiments.

### A. Signal in uncorrelated noise

In our first experiment, we consider the classical Example 1 as defined in (2)-(3). We compare three detectors:

- GLRT: Assuming Gaussian noise, the classical GLRT has a simple closed form solution  $T_{\text{GLRT}} = (\mathbf{x}^T \mathbf{1})^2 / (\mathbf{x}^T \mathbf{x})$  and is known to be CFAR.
- NET: A learned neural network as in Algorithm 1. We choose a uniform fake prior for the unknown parameters in (3). The architecture is based on four non-linear features: the sample mean of  $\mathbf{x}$ , its sample variance and robust versions of the two based on the median. These

features are passed through a fully connected neural network, and are optimized to minimize a cross entropy loss using PyTorch.

- CFARnet: A learned neural network as in Algorithm 2. Architecture and implementation are all identical to NET. Loss is cross entropy with an MMD CFAR penalty with parameter  $\alpha = 1$ .

The first experiment considers Gaussian noise. In the first row of Fig. 1, we plot the two ROCs for different values of  $\sigma$ . To examine the CFAR property, we also plot the FPRs under different parameters. As expected, it is easy to see that the Gaussian GLRT performs well and is CFAR. NET provides similar accuracy as illustrated in its ROC but is non-CFAR and results in significantly different FPR when we change  $\sigma$ . On the other hand, CFARnet is both accurate and near CFAR.

The next setup is more challenging and considers non-Gaussian noise. The setting is identical as before except for the noise distribution

$$p(n_k) = (1 - \epsilon)N(0, 1) + \epsilon N(0, 100) \quad (37)$$

where  $\epsilon = 0.1$ . This setting represents a Gaussian noise with outliers. There is no simple GLRT for this setting. The results are provided in the second row of Fig. 1. In this case, the Gaussian GLRT is no longer optimal and the two learned detectors provide a significantly better ROC. In terms of CFAR, GLRT is still invariant to the nuisance parameter, but the FPR of NET is dependent on its value. As argued, CFARnet is both accurate and CFAR.

### B. Gaussian signal in correlated noise

In our second experiment, we consider the detection of a known signal  $\mathbf{s}$  with unknown amplitude in Gaussian noise with unknown covariance  $\Sigma$ . This is a classical problem in adaptive target detection [27, 28]. Following these works, we assume a secondary data of  $n$  i.i.d. noise-only samples  $\mathbf{x}_{aux} = (\mathbf{w}_1, \dots, \mathbf{w}_n)$ . Together the observations can be modelled as

$$\begin{aligned} \mathbf{x} &= A\mathbf{s} + \mathbf{w}_0 \\ \mathbf{x}_i &= \mathbf{w}_i \quad i = 1, \dots, n \end{aligned} \quad (38)$$

where

$$\mathbf{w}_0, \mathbf{w}_i \sim \mathcal{N}(\mathbf{0}, \Sigma) \quad (39)$$

The vector  $\mathbf{z}$  includes both  $A$  and all the elements in the matrix  $\Sigma$ . The goal is to decide between

$$\begin{aligned} y = 0 : & \quad A = 0 \\ y = 1 : & \quad A \neq 0. \end{aligned} \quad (40)$$

The classical adaptive matched filter (AMF) detector is GLRT where the unknown covariance matrix is replaced by its sample covariance [28]:

$$T_{\text{AMF}}(\mathbf{x}) = \frac{(\mathbf{s}^T \hat{\Sigma}^{-1} \mathbf{x})^2}{\mathbf{s}^T \hat{\Sigma}^{-1} \mathbf{s}} \quad (41)$$

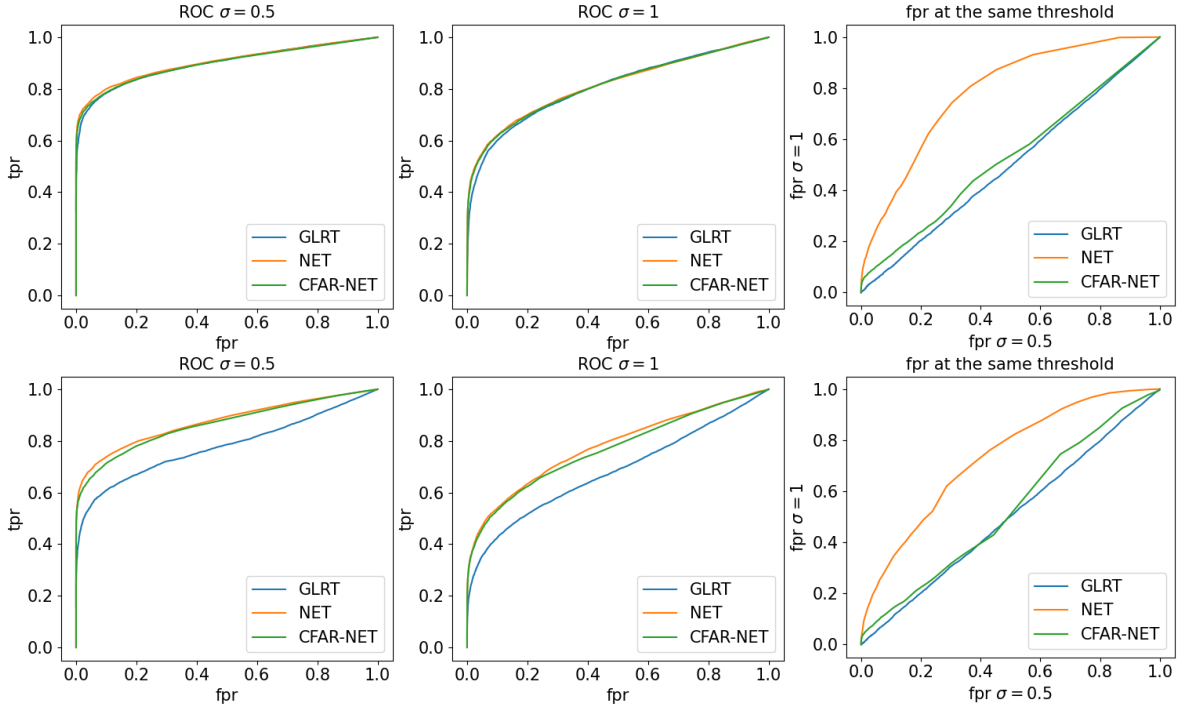


Fig. 1. Performance graphs in terms of FPR, TPR and thresholds for  $\sigma \in \{0, 1\}$ . Top row is with Gaussian noise and indeed the Gaussian GLRT is best both in terms of ROC and CFAR. NET succeeds in achieving its ROC but is not CFAR. CFARnet is both accurate and CFAR. Bottom row is with non-Gaussian noise and the learned detectors beat the Gaussian GLRT in accuracy. CFARnet is near CFAR with a slight decrease in accuracy, but again is approximately CFAR

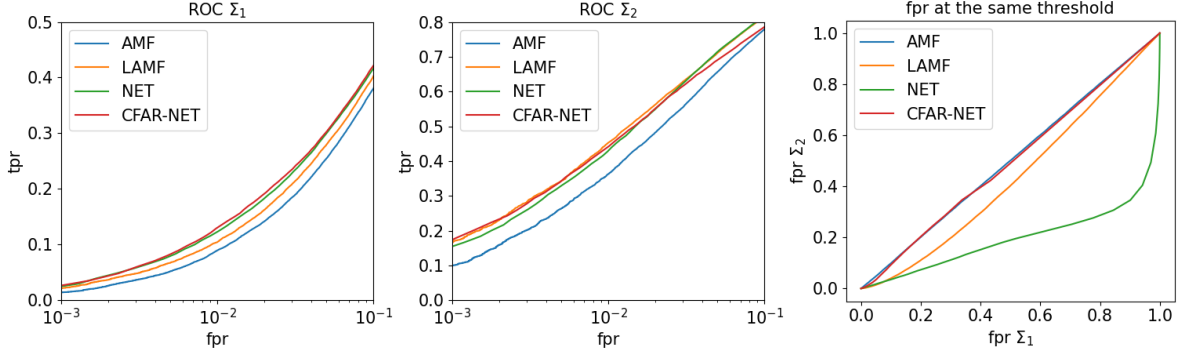


Fig. 2. Performance graphs in terms of FPR, TPR and thresholds for two different values of  $\Sigma$ . LAMF, NET and CFARnet are better than AMF (especially at the interesting low-FPR regime). Unlike CFARnet, the LAMF and NET are highly non-CFAR.

with

$$\hat{\Sigma} = \frac{1}{n} \sum_{i=1}^n \mathbf{w}_i \mathbf{w}_i^T. \quad (42)$$

See also the related detector due to Kelly [27]:

$$T_{\text{Kelly}}(\mathbf{x}) = \frac{(\mathbf{s}^T \hat{\Sigma}^{-1} \mathbf{x})^2}{(\mathbf{s}^T \hat{\Sigma}^{-1} \mathbf{s})(1 + \mathbf{x}^T \hat{\Sigma}^{-1} \mathbf{x})}. \quad (43)$$

The AMF in (41) is CFAR but is sub-optimal when  $n$  is small. In such settings, it is preferable to plug in regularized covariance estimators:

$$\hat{\Sigma}_\lambda = \hat{\Sigma} + \lambda \mathbf{I}. \quad (44)$$

This leads to the popular diagonally loaded LAMF which is generally not CFAR [36, 37].

To design a CFAR version of the above detectors, we train a fully connected model with a single hidden layer with the following features as inputs:

$$\begin{aligned} f_1^\lambda(\mathbf{x}) &= \mathbf{s}^T \hat{\Sigma}_\lambda^{-1} \mathbf{x} \\ f_2^\lambda(\mathbf{x}) &= \mathbf{s}^T \hat{\Sigma}_\lambda^{-1} \mathbf{s} \\ f_3^\lambda(\mathbf{x}) &= \mathbf{x}^T \hat{\Sigma}_\lambda^{-1} \mathbf{x}. \end{aligned} \quad (45)$$

We use 10 different values of  $\lambda$  between 0 and 0.3. The input to the neural network in this case is a concatenation of all 30 features to a single vector. Fig. 2 shows the ROC curves

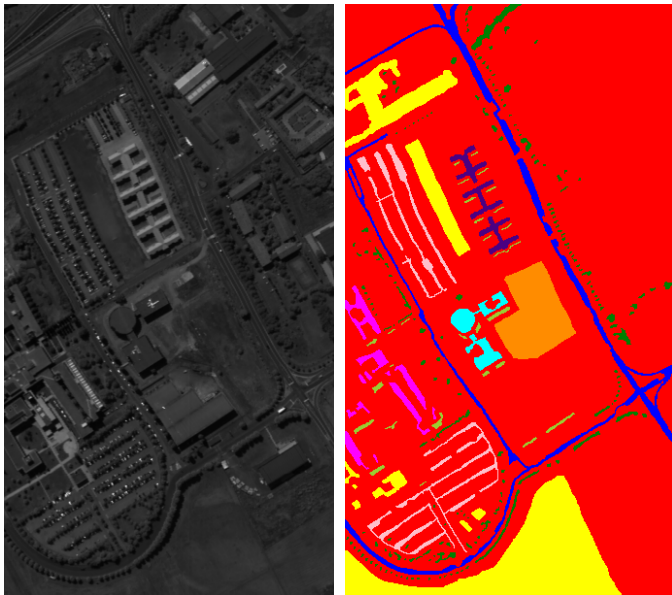


Fig. 3. Illustration of Pavia University dataset. Left is a grayscale image that was generated using the sum of all the channels and in right is a map of the materials annotation.

of AMF, LAMF with  $\lambda = 0.03$ , NET and CFARnet on two different covariances. We also plot the FPRs under different parameters. The performance of LAMF, NET and CFARnet are better than AMF (especially at the interesting low-FPR regime). While LAMF and NET are far from CFAR, CFARnet is approximately CFAR.

### C. Target detection in real-world hyperspectral image

The main motivation to CFARnet is training detectors using a synthetic dataset with continuous large scale parameters. For completeness, our last experiment considers the use of CFARnet in a (semi) real world setting with a finite valued nuisance parameter. Specifically, we consider target detection in real hyperspectral images annotated according to a finite number of materials. The image is taken from the Pavia University dataset (Fig. 3). Fifth of the pixels are annotated to be one of nine materials, e.g., asphalt or trees. We use these annotations as the unknown  $\mathbf{z}$  parameters. Following [11], we synthetically plant artificial targets on the real image. The target’s spectrum is taken from the USGS Spectral Library [14] and is interpolated to fit the 103 bands of the hyperspectral image. It is planted randomly (with probability of a half) in the image using an additive model:

$$\mathbf{x} = \alpha \mathbf{t} + \mathbf{v} \quad (46)$$

where  $\mathbf{v}$  is the original pixel vector,  $\mathbf{t}$  is the target and  $\alpha = 0.05$  is the amplitude of the target. We use two thirds of the data for training and the rest for testing.

We train a simple fully-connected neural network with two hidden layers. First, we fit NET using a standard cross entropy loss and then using CFARnet. To overcome the imbalance between the number of examples of each material, in each

TABLE I  
PARTIAL AUC IN  $(0 - 0.05)$  OF TPR AS A FUNCTION OF THE WORST CASE FPR. IN ALL LABELED MATERIALS CFARNET OUTPERFORMS NET.

MATERIAL	NET	CFARNET
UNLABELED	<b>0.49</b>	0.47
1	0.31	<b>0.38</b>
2	0.74	<b>0.77</b>
3	0.33	<b>0.35</b>
4	0.69	<b>0.73</b>
5	0.27	<b>0.34</b>
6	0.49	<b>0.53</b>
7	0.47	<b>0.72</b>
8	0.41	<b>0.49</b>
9	0.88	<b>0.9</b>

step of the stochastic gradient descent, we randomly choose one material and generate a batch for it. Fig. 4 shows that while NET is better in terms of ROC curve, it is far from CFAR. CFARnet shows an expected degradation in performance but is approximately CFAR. To get additional insight on the price of CFAR, we also consider a natural baseline that uses NET but computes its threshold to guarantee a required FPR constraint on the worst case material. Table I compares the partial AUC of the TPR as a function of the worst case FPR in  $(0 - 0.05)$ . It can be seen that in all materials except the unlabeled, CFARnet is better with respect to this metric.

## VII. DISCUSSION AND FUTURE WORK

In recent years, deep neural networks are replacing classical algorithms for detection in many fields. While deep neural networks give remarkable improvements in accuracy, they lack important properties as CFAR. In this paper we proposed a method to train CFAR neural networks.

Additional research is required to analyze the theoretical and practical decrease in accuracy due to the CFAR constraint. In addition, we proved that CFARnet converges to GLRT in asymptotic linear Gaussian settings. It will be interesting to explore similar properties in more practical setups. Finally, another important direction for future work is to apply the proposed method on large scale and real world problems.

### ACKNOWLEDGMENT

The authors would like to thank Yoav Wald for fruitful discussions and helpful insights. This research was partially supported by ISF grant number 2672/21.

### APPENDIX

#### A. Statistical distances and MMD

In this appendix, we provide with a brief background on statistical distances. Maximum Mean Discrepancy (MMD) is an integral probability metric defined as [26]:

$$d_{\text{MMD}}(X; Y) = \mathbf{E}[k(X, X')] + \mathbf{E}[k(Y, Y')] - 2\mathbf{E}[k(X, Y)] \quad (47)$$

where  $X$  and  $X'$  are independent and identically distributed (i.i.d.), and so are  $Y$  and  $Y'$ . The function  $k(\cdot, \cdot)$  is a

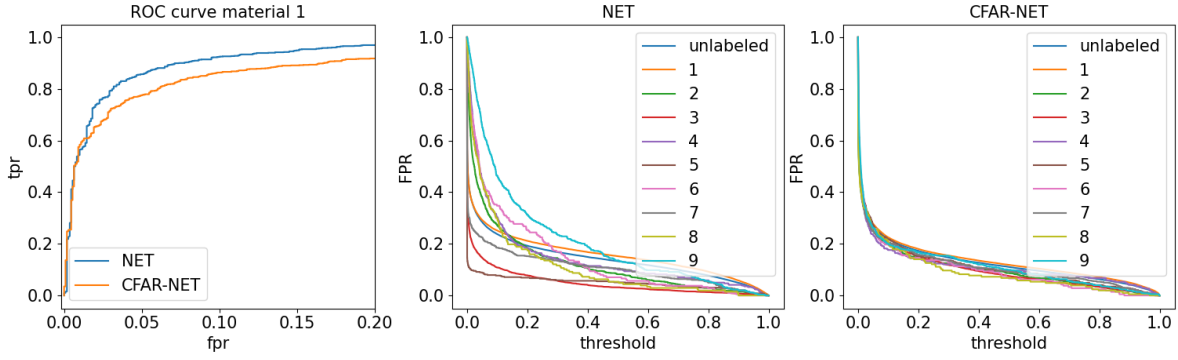


Fig. 4. Performance graphs in terms of FPR, TPR and threshold. The left plot shows the ROC curve for one of the materials. The two right plots show the FPR as a function of the threshold for in each material. While NET is better in terms of ROC curve, it is far from CFAR, while CFARnet is approximately CFAR

characteristic kernel over a reproducing kernel Hilbert space, e.g., the Gaussian Radial Basis Function (RBF).

Recent advances in deep generative models allow us to optimize distances as MMD in an empirical and differentiable manner [25]. For this purpose, we need to represent each distribution using a small dataset. Let  $\{X_i\}_{i=1}^N$  and  $\{Y_i\}_{i=1}^N$  be i.i.d. realizations of  $X$  and  $Y$ , respectively. Then, an empirical version of the MMD can be used where the expectations in (47) are replaced by their empirical estimates. More advanced metrics can be obtained using the tools of generative adversarial networks (GANs). In this paper, we only deal with distances between scalar random variables and simple MMD distances suffice.

### B. LRT of linear model with a random signal

In this appendix we derive the LRT of linear model with a random signal  $\mathbf{z}_r \sim \mathcal{N}(\mathbf{0}, \sigma_r^2 \mathbf{I})$  and known covariance  $\Sigma$ . Again, a similar derivation can be found in [16]. The distribution of signal with noise is  $\mathcal{N}(\mathbf{0}, \Sigma + \sigma_r^2 \mathbf{H}\mathbf{H}^T)$  and thus the LRT (after taking the log and multiplying by 2) is:

$$T_{\text{PBL}}(\mathbf{x}) = \mathbf{x}^T \left( \Sigma^{-1} - (\Sigma + \sigma_r^2 \mathbf{H}\mathbf{H}^T)^{-1} \right) \mathbf{x} + \log \left( \frac{\det \Sigma}{\det(\Sigma + \sigma_r^2 \mathbf{H}\mathbf{H}^T)} \right) \quad (48)$$

Using the matrix inversion lemma,

$$\begin{aligned} \Sigma^{-1} - (\Sigma + \sigma_r^2 \mathbf{H}\mathbf{H}^T)^{-1} &= \\ &= \Sigma^{-1} - \Sigma^{-1} \\ &+ \Sigma^{-1} \mathbf{H} \left( \mathbf{H}^T \Sigma^{-1} \mathbf{H} + \frac{1}{\sigma_r^2} \mathbf{I} \right)^{-1} \mathbf{H}^T \Sigma^{-1} \\ &= \Sigma^{-1} \mathbf{H} \left( \mathbf{H}^T \Sigma^{-1} \mathbf{H} + \frac{1}{\sigma_r^2} \mathbf{I} \right)^{-1} \mathbf{H}^T \Sigma^{-1}. \end{aligned} \quad (49)$$

Finally, plugging (49) into (48) yields:

$$T_{\text{PBL}}(\mathbf{x}) = \mathbf{x}^T \Sigma^{-1} \mathbf{H} \left( \mathbf{H}^T \Sigma^{-1} \mathbf{H} + \frac{1}{\sigma_r^2} \mathbf{I} \right)^{-1} \mathbf{H}^T \Sigma^{-1} \mathbf{x} + \log \left( \frac{\det \Sigma}{\det(\Sigma + \sigma_r^2 \mathbf{H}\mathbf{H}^T)} \right). \quad (50)$$

### C. GLRT for linear model with known covariance

In this appendix, we derive the GLRT for an unknown  $\mathbf{z}_r$ . A similar derivation can be found in [16].

The likelihood of linear model is given by:

$$p(\mathbf{x} | \mathbf{z}_n, \Sigma) = \frac{1}{(2\pi)^{\frac{n}{2}} \det(\Sigma)^{\frac{1}{2}}} e^{-\frac{1}{2}(\mathbf{x} - \mathbf{H}\mathbf{z}_r)^T \Sigma^{-1} (\mathbf{x} - \mathbf{H}\mathbf{z}_r)} \quad (51)$$

The LRT for known  $\mathbf{z}_n$  is therefore (after taking the log and multiplying by 2):

$$T_{\text{LRT}}(\mathbf{x}) = 2\mathbf{x}^T \Sigma^{-1} \mathbf{H}\mathbf{z}_r - \mathbf{z}_r^T \mathbf{H}^T \Sigma^{-1} \mathbf{H}\mathbf{z}_r. \quad (52)$$

When  $\mathbf{z}_r$  is unknown, its ML estimator is given by the weighted least squares estimator [38, p. 226]:

$$\hat{\mathbf{z}}_r = \left( \mathbf{H}^T \Sigma^{-1} \mathbf{H} \right)^{-1} \mathbf{H}^T \Sigma^{-1} \mathbf{x}. \quad (53)$$

Plugging (53) into (52) yields:

$$\begin{aligned} T_{\text{GLRT}} &= 2\mathbf{x}^T \Sigma^{-1} \mathbf{H} \left( \mathbf{H}^T \Sigma^{-1} \mathbf{H} \right)^{-1} \mathbf{H}^T \Sigma^{-1} \mathbf{x} \\ &- \mathbf{x}^T \Sigma^{-1} \mathbf{H} \left( \mathbf{H}^T \Sigma^{-1} \mathbf{H} \right)^{-1} \mathbf{H}^T \Sigma^{-1} \mathbf{x} \\ &= \mathbf{x}^T \Sigma^{-1} \mathbf{H} \left( \mathbf{H}^T \Sigma^{-1} \mathbf{H} \right)^{-1} \mathbf{H}^T \Sigma^{-1} \mathbf{x} \end{aligned} \quad (54)$$

### D. Asymptotic performance of GLRT of linear model

In this appendix, we prove the following lemma:

**Lemma 1.** *The GLRT of the linear model with Gaussian noise in (16)- (18) attains its asymptotic distribution for any signal strength (unlike the more general case that requires a weak signal assumption).*

*Proof.* Let

$$\mathbf{F}(\mathbf{z}_r, \mathbf{z}_n) = \begin{pmatrix} \mathbf{F}_{\mathbf{z}_r \mathbf{z}_r} & \mathbf{F}_{\mathbf{z}_r \mathbf{z}_n} \\ \mathbf{F}_{\mathbf{z}_n \mathbf{z}_r} & \mathbf{F}_{\mathbf{z}_n \mathbf{z}_n} \end{pmatrix} \quad (55)$$

be the Fisher Information Matrix associated with the parameters  $\mathbf{z}_r$  and  $\mathbf{z}_n$ . Due to the Gaussian distribution, the matrix has a well known form as detailed in [38, p. 47]. In our case, the mean depends linearly on  $\mathbf{z}_r$ , the mean does not depend on  $\mathbf{z}_n$  and the covariance does not depend on  $\mathbf{z}_r$ . Thus, it is

easy to verify that the matrix and its sub-blocks satisfy three properties:

$$\mathbf{F}_{\mathbf{z}_r \mathbf{z}_r}(\alpha \mathbf{z}_r, \mathbf{z}_n) = \mathbf{F}_{\mathbf{z}_r \mathbf{z}_r}(\mathbf{z}_r, \mathbf{z}_n) \quad \forall \quad \alpha > 0 \quad (56)$$

$$\mathbf{F}_{\mathbf{z}_n \mathbf{z}_n}(\mathbf{z}_r, \mathbf{z}_n) = \text{function}(\mathbf{z}_n) \quad (57)$$

$$\mathbf{F}_{\mathbf{z}_r \mathbf{z}_n}(\mathbf{z}_r, \mathbf{z}_n) = 0. \quad (58)$$

Now, consider a linear model where the true parameter vector  $\mathbf{z}_r$  is parameterized by a strength  $\alpha$ , that is  $\mathbf{z}_r^\alpha = \alpha \mathbf{z}_r$ . Denote the GLRT for  $\mathbf{z}_r^\alpha$  with known  $\mathbf{z}_n$  by  $T_{\text{known}}(\alpha)$ . Examining the structure in (21) reveals that

$$\alpha^2 T_{\text{known}}(\alpha) \stackrel{\text{asympt}}{\sim} T_{\text{known}}(1) \quad (59)$$

Next, denote the GLRT for  $\mathbf{z}_r^\alpha$  with unknown  $\mathbf{z}_n$  by  $T_{\text{unknown}}(\alpha)$ . In this case,  $\alpha$  may also affect the estimation of the unknown covariance. Fortunately, due to (57), the errors are independent of  $\mathbf{z}_r$ , and we also have

$$\alpha^2 T_{\text{unknown}}(\alpha) \stackrel{\text{asympt}}{\sim} T_{\text{unknown}}(1) \quad (60)$$

For  $\alpha \rightarrow 0$ , the asymptotic distributions are  $\chi_r'(\lambda)$  with [16, p. 206]:

$$\lambda_{\text{known}} = \mathbf{z}_r^{\alpha T} \mathbf{F}_{\mathbf{z}_r^\alpha \mathbf{z}_r^\alpha} \mathbf{z}_r^\alpha = \alpha^2 \mathbf{z}_r^T \mathbf{F}_{\mathbf{z}_r \mathbf{z}_r} \mathbf{z}_r \quad (61)$$

and

$$\lambda_{\text{unknown}} = \mathbf{z}_r^{\alpha T} (\mathbf{F}_{\mathbf{z}_r^\alpha \mathbf{z}_r^\alpha} - \mathbf{F}_{\mathbf{z}_n \mathbf{z}_n} \mathbf{F}_{\mathbf{z}_n \mathbf{z}_n}^{-1} \mathbf{F}_{\mathbf{z}_n \mathbf{z}_n} \mathbf{F}_{\mathbf{z}_n \mathbf{z}_n} \mathbf{z}_r^\alpha) \mathbf{z}_r^\alpha \quad (62)$$

where  $\chi'$  is the noncentral chi-squared distribution. Due to (58), we have that  $\lambda_{\text{known}} = \lambda_{\text{unknown}}$  for  $\alpha \rightarrow 0$ .

Finally, this means that the asymptotic properties hold for arbitrary  $\mathbf{z}_r$  (corresponding to  $\alpha = 1$ )

$$T_{\text{unknown}}(1) \stackrel{\text{asympt}}{\sim} \alpha^2 T_{\text{unknown}}(\alpha) \stackrel{\text{asympt}}{\sim} \alpha^2 T_{\text{known}}(\alpha) \stackrel{\text{asympt}}{\sim} T_{\text{known}}(1). \quad (63)$$

□

## REFERENCES

- [1] C. Dong, C. C. Loy, K. He, and X. Tang, “Image super-resolution using deep convolutional networks,” *IEEE transactions on pattern analysis and machine intelligence*, vol. 38, no. 2, pp. 295–307, 2015.
- [2] G. Ongie, A. Jalal, C. A. Metzler, R. G. Baraniuk, A. G. Dimakis, and R. Willett, “Deep learning techniques for inverse problems in imaging,” *IEEE Journal on Selected Areas in Information Theory*, vol. 1, no. 1, pp. 39–56, 2020.
- [3] L. Gabrielli, S. Tomassetti, S. Squartini, and C. Zinato, “Introducing deep machine learning for parameter estimation in physical modelling,” in *Proceedings of the 20th International Conference on Digital Audio Effects*, 2017.
- [4] V. Dua, “An artificial neural network approximation based decomposition approach for parameter estimation of system of ordinary differential equations,” *Computers & chemical engineering*, vol. 35, no. 3, 2011.
- [5] R. Dreifuerst and R. W. Heath Jr, “SignalNet: A low resolution sinusoid decomposition and estimation network,” *arXiv preprint arXiv:2106.05490*, 2021.
- [6] T. Diskin, Y. C. Eldar, and A. Wiesel, “Learning to estimate without bias,” *Preprint arXiv:2110.12403*, 2021.
- [7] N. Samuel, T. Diskin, and A. Wiesel, “Learning to detect,” *IEEE Transactions on Signal Processing*, vol. 67, no. 10, pp. 2554–2564, 2019.
- [8] L. Girard, V. Roy, P. Giguère, and T. Eude, “Deep neural network training using synthetic signatures for rare target detection in SWIR hyperspectral imagery,” in *2021 IEEE International Geoscience and Remote Sensing Symposium IGARSS*, pp. 4420–4423, IEEE, 2021.
- [9] A. Brighente, F. Formaggio, G. M. Di Nunzio, and S. Tomasin, “Machine learning for in-region location verification in wireless networks,” *IEEE Journal on Selected Areas in Communications*, vol. 37, no. 11, pp. 2490–2502, 2019.
- [10] D. de la Mata-Moya, M. P. Jarabo-Amores, J. M. de Nicolás, and M. Rosa-Zurera, “Approximating the Neyman–Pearson detector with 2C-SVMs. application to radar detection,” *Signal Processing*, vol. 131, pp. 364–375, 2017.
- [11] A. Ziemann, M. Kucer, and J. Theiler, “A machine learning approach to hyperspectral detection of solid targets,” in *Algorithms and Technologies for Multispectral, Hyperspectral, and Ultraspectral Imagery XXIV*, vol. 10644, p. 1064404, International Society for Optics and Photonics, 2018.
- [12] J. Theiler, S. Matteoli, and A. Ziemann, “Bayesian detection of solid subpixel targets,” in *2021 IEEE International Geoscience and Remote Sensing Symposium IGARSS*, pp. 3213–3216, IEEE, 2021.
- [13] E. Conte, A. De Maio, and C. Galdi, “CFAR detection of multidimensional signals: An invariant approach,” *IEEE Transactions on Signal Processing*, vol. 51, no. 1, pp. 142–151, 2003.
- [14] R. Kokaly, R. Clark, G. Swayze, K. Livo, T. Hoefen, N. Pearson, R. Wise, W. Benzel, H. Lowers, R. Driscoll, *et al.*, “USGS spectral library version 7 data: US geological survey data release,” *United States Geological Survey (USGS): Reston, VA, USA*, 2017.
- [15] A. Coluccia, A. Fascista, and G. Ricci, “Design of customized adaptive radar detectors in the CFAR feature plane,” *arXiv preprint arXiv:2203.12565*, 2022.
- [16] S. Kay, *Fundamentals of Statistical Signal Processing: Detection theory*. Fundamentals of Statistical Si, Prentice-Hall PTR, 1998.
- [17] A. Herschtal and B. Raskutti, “Optimising area under the ROC curve using gradient descent,” in *Proceedings of the twenty-first international conference on Machine learning*, p. 49, 2004.
- [18] U. Brefeld, T. Scheffer, *et al.*, “AUC maximizing support vector learning,” in *Proceedings of the ICML 2005 workshop on ROC Analysis in Machine Learning*, 2005.
- [19] H. Narasimhan and S. Agarwal, “A structural SVM based approach for optimizing partial AUC,” in *International Conference on Machine Learning*, pp. 516–524, PMLR, 2013.

- [20] P. Braca, L. M. Millefiori, A. Aubry, S. Marano, A. De Maio, and P. Willett, "Statistical hypothesis testing based on machine learning: Large deviations analysis," *arXiv preprint arXiv:2207.10939*, 2022.
- [21] C.-H. Lin, Y.-C. Lin, Y. Bai, W.-H. Chung, T.-S. Lee, and H. Huttunen, "DL-CFAR: A novel cfar target detection method based on deep learning," in *2019 IEEE 90th Vehicular Technology Conference (VTC2019-Fall)*, pp. 1–6, IEEE, 2019.
- [22] J. Akhtar and K. E. Olsen, "A neural network target detector with partial CA-CFAR supervised training," in *2018 International Conference on Radar (RADAR)*, pp. 1–6, IEEE, 2018.
- [23] J. Akhtar, "Training of neural network target detectors mentored by SO-CFAR," in *2020 28th European Signal Processing Conference (EUSIPCO)*, pp. 1522–1526, IEEE, 2021.
- [24] I. Goodfellow, J. Pouget-Abadie, M. Mirza, B. Xu, D. Warde-Farley, S. Ozair, A. Courville, and Y. Bengio, "Generative adversarial nets," *Advances in neural information processing systems*, vol. 27, 2014.
- [25] Y. Li, K. Swersky, and R. Zemel, "Generative moment matching networks," in *International conference on machine learning*, pp. 1718–1727, PMLR, 2015.
- [26] A. Gretton, K. M. Borgwardt, M. J. Rasch, B. Schölkopf, and A. Smola, "A kernel two-sample test," *The Journal of Machine Learning Research*, vol. 13, no. 1, pp. 723–773, 2012.
- [27] E. J. Kelly, "An adaptive detection algorithm," *IEEE transactions on aerospace and electronic systems*, no. 2, pp. 115–127, 1986.
- [28] F. C. Robey, D. R. Fuhrmann, E. J. Kelly, and R. Nitzberg, "A CFAR adaptive matched filter detector," *IEEE Transactions on aerospace and electronic systems*, vol. 28, no. 1, pp. 208–216, 1992.
- [29] E. Conte, M. Lops, and G. Ricci, "Adaptive matched filter detection in spherically invariant noise," *IEEE Signal Processing Letters*, vol. 3, no. 8, pp. 248–250, 1996.
- [30] D. G. Manolakis, C. Siracusa, D. Marden, and G. A. Shaw, "Hyperspectral adaptive matched-filter detectors: Practical performance comparison," in *Algorithms for Multispectral, Hyperspectral, and Ultraspectral Imagery VII*, vol. 4381, pp. 18–33, SPIE, 2001.
- [31] M. Arjovsky, L. Bottou, I. Gulrajani, and D. Lopez-Paz, "Invariant risk minimization," *arXiv preprint arXiv:1907.02893*, 2019.
- [32] Y. Wald, A. Feder, D. Greenfeld, and U. Shalit, "On calibration and out-of-domain generalization," *arXiv preprint arXiv:2102.10395*, 2021.
- [33] Y. Romano, S. Bates, and E. Candes, "Achieving equalized odds by resampling sensitive attributes," *Advances in Neural Information Processing Systems*, vol. 33, pp. 361–371, 2020.
- [34] P. L. Bartlett, M. I. Jordan, and J. D. McAuliffe, "Convexity, classification, and risk bounds," *Journal of the American Statistical Association*, vol. 101, no. 473, pp. 138–156, 2006.
- [35] A. Yeredor, "The joint MAP-ML criterion and its relation to ml and to extended least-squares," *IEEE Transactions on Signal Processing*, vol. 48, no. 12, pp. 3484–3492, 2000.
- [36] O. Ledoit and M. Wolf, "A well-conditioned estimator for large-dimensional covariance matrices," *Journal of multivariate analysis*, vol. 88, no. 2, pp. 365–411, 2004.
- [37] Y. I. Abramovich, N. K. Spencer, and A. Y. Gorokhov, "Modified GLRT and AMF framework for adaptive detectors," *IEEE Transactions on Aerospace and Electronic Systems*, vol. 43, no. 3, pp. 1017–1051, 2007.
- [38] S. M. Kay and S. M. Kay, *Fundamentals of statistical signal processing: estimation theory*, vol. 1. Prentice-hall Englewood Cliffs, NJ, 1993.